

PCCP

Accepted Manuscript



This is an *Accepted Manuscript*, which has been through the Royal Society of Chemistry peer review process and has been accepted for publication.

Accepted Manuscripts are published online shortly after acceptance, before technical editing, formatting and proof reading. Using this free service, authors can make their results available to the community, in citable form, before we publish the edited article. We will replace this *Accepted Manuscript* with the edited and formatted *Advance Article* as soon as it is available.

You can find more information about *Accepted Manuscripts* in the [Information for Authors](#).

Please note that technical editing may introduce minor changes to the text and/or graphics, which may alter content. The journal's standard [Terms & Conditions](#) and the [Ethical guidelines](#) still apply. In no event shall the Royal Society of Chemistry be held responsible for any errors or omissions in this *Accepted Manuscript* or any consequences arising from the use of any information it contains.

ARTICLE

Durable Surface-enhanced Raman Scattering Substrate: Ultrathin Carbon Layer Encapsulated Ag Nanoparticle Arrays on Indium-Tin-Oxide Glass

Cite this: DOI: 10.1039/x0xx00000x

Received 00th January 2012,

Accepted 00th January 2012

DOI: 10.1039/x0xx00000x

www.rsc.org/

Juncao Bian,^a Qian Li,^b Chao Huang,^a Yao Guo,^a Myowin Zaw,^a Rui-Qin Zhang*^a

The application of Ag nanostructures to surface-enhanced Raman scattering (SERS) is hindered by their chemical instability. Fabrication of durable Ag-based SERS substrates is therefore of great significance in practical applications. In this work, ultrathin C-layer-encapsulated Ag nanoparticle arrays (UCL-Ag-NA) are successfully fabricated on the surface of indium-tin-oxide (ITO) glass, using a hydrothermal method, for use as durable SERS substrates. The problem of Ag nanoparticles dissolving during the hydrothermal process is solved by using ZnO powders as a pH-buffering reagent. The SERS signal intensity from UCL-Ag-NA decreases, accompanied by an improved Raman signal stability, as the C-layer thickness increases. Raman spectra show that the SERS signal intensities obtained from UCL-Ag-NA with C-layers of 4.5 nm and 7.3 nm stored for 180 days are 64.9% and 77.8% of those obtained from as-prepared counterparts. The SERS intensity of the UCL-Ag-NA (C-layer of 4.5 nm) is 152.7% that of the bare Ag NA after 180 days storage. XPS spectra confirm that the C-layer effectively suppresses the oxidation of the Ag NA. This methodology can be generalized to improve the durability of other dimensional Ag nanostructures for SERS applications.

1. Introduction

Localized surface plasmons (LSP) have received considerable attention due to their potential applications in optics,¹ light-emitting devices,² solar cells,³ surface-enhanced Raman scattering (SERS),⁴ and so on. Of these areas, SERS is a reliable spectroscopic analytical tool for the detection and structural analysis of organic molecules, even down to single molecule level.⁴ The high sensitivity of this technique, by absorbing the target species on the vicinity of plasmonic nanostructures, can be mainly attributed to the strong local electric field at the narrow gaps and sharp tips (termed hot spots).⁵ To date, Ag and Au have been the most widely investigated systems for SERS. The enhancement factor of Ag is about two orders of magnitude larger than that of Au for the same nanostructure.^{6,7} Substrate-supported Ag nanostructures are of great interest as they exhibit much better signal reproducibility than their solution-dispersed counterparts.⁷⁻¹¹ However, nanosilver is easily oxidized, even in ambient conditions. The thickness of the Ag_xO shell layer increases with time, which can decrease the surface electric fields. As a result, the enhancement ability of the Ag-based SERS substrate is weakened. Therefore, the durability of the Ag-based SERS substrate is a key issue in advancing its practical applications.

To improve the stability of Ag nanostructures, a shell layer is always encapsulated on their surface. These materials include TiO₂,¹² Al₂O₃,¹³ SiO₂,¹³ diamond,¹⁴ graphene,¹⁵ and amorphous C.¹⁶ To avoid pinholes, the shell layer is always thick and may even be thicker than the core itself. Due to the near-field nature of SERS, too thick a shell layer would seriously decrease the sensitivity of the substrate. Tian proposes a shell-isolated, nanoparticle-enhanced Raman spectroscopy by using atom layer deposition (ALD) to deposit an ultrathin (~2 nm) Al₂O₃ or SiO₂ layer on the surface of Au nanoparticles.¹³ ALD can allow accurate control of the thickness

of the shell layer on the surface of metallic nanostructures. However, it requires expensive equipment and the efficiency is very low for large-scale production. Qu reports a sample of single-layer, graphene-protected Ag nanoparticles which shows good stability.¹⁴ Single-layer graphene has less of a damping effect than other materials on the surface plasmons of Ag nanostructures due to its extreme thinness. However, its synthesis requires a high temperature (up to 1000 °C), so scaling up the production of single-layer graphene-protected Ag nanostructures as a SERS substrate is expensive. In contrast, using the hydrothermal method, as reported by Chen,¹⁶ to fabricate thin C-layers on the surface of Ag nanoparticles is cost-effective and easy to manipulate.

In this work, a hydrothermal methodology is used to encapsulate Ag nanostructures with an ultrathin C-layer (UCL). After 180 days, UCL-encapsulated Ag nanoparticle arrays (UCL-Ag-NA) exhibit relatively stable SERS enhancement ability, indicating that the proposed technique can be used to fabricate durable Ag-based SERS substrates. It is found that the Ag nanostructures corroded under the hydrothermal conditions, which has rarely been reported. This corrosion problem reduces the enhancement ability of the as-prepared Ag nanostructures on a solid substrate. In the present work, by adding a buffering reagent, namely ZnO powder, the UCL was successfully deposited on the surface of the Ag nanoparticles. This largely suppressed the corrosion problem under hydrothermal conditions.

2. Experimental details

All the reagents were purchased from Acros except as otherwise stated. Ag nanoparticle arrays (Ag NA) were electrodeposited on indium-tin-oxide (ITO) glass using a double-potentiostatic method.⁹ 300 mL of electrolyte containing 0.5 mM AgNO₃ and 0.1 M KNO₃

was obtained by adding 15 mL of 10 mM AgNO₃ and 30 mL of 1 M KNO₃ to 255 mL of MiliQ water (18.2 MΩ). Electrodeposition was carried out in a three-electrode system (electrochemistry workstation by Wuhan Gauss Union Co. Ltd.). ITO glass, Pt plate (2 mm × 5 mm × 0.1 mm) and a saturate calomel electrode (SCE) were used as the working, counter, and reference electrodes, respectively. To avoid the contamination of Cl⁻ from the SCE, the electrolyte and SCE were separated by a U-shaped salt bridge filled with gelatinized saturated KNO₃ and agar solution. The SCE was inserted in the saturated KNO₃ solution. All the potentials in this work are stated by reference to the SCE. 40 mL of electrolyte was used each time. The nucleation potential was -0.3V, aging for 50 s, and the growth potential was -0.02 V, kept for 1200 s. Then Ag NA were deposited on the surface of ITO glass. After electrodeposition, the samples were rinsed with MiliQ water and dried off in N₂.

ZnO powders were synthesized using a reported chemical bath method.¹⁷ 10 mL of 0.5 M Zn(NO₃)₂, 1.65 g of hexamethylenetetramine (HMT) and 0.8 mL of polyethyleneimine (PEI, Beijing Midwest Group, Beijing, China) were added to 50 mL of MiliQ water. After stirring for 1 h at 30 °C, the solution was moved to an oven and kept at 95 °C for 3 h. The powders were then centrifuged at 5000 rpm and cleaned with MiliQ water three times and once again by ethanol. They were dried in the oven at 80 °C for 2 h and stored for use.

For the UCL, the method of Chen¹⁶ was used with some modification. 0.15 g of glucose and 0.04 g of ZnO powder were added to 10 mL of MiliQ water. After stirring for 10 min, the solution was ultrasonically treated for 5 min to disperse the ZnO powder, then stirred for another 5 min and transferred to Teflon (23 mL). A piece of ITO glass with Ag NA was put against the inner wall of the Teflon, with the Ag NA facing down. The Teflon was then moved to the oven at 150 °C. Growth time was changed to fine-

tune the thickness of the C-layer on the surface of the Ag nanoparticles. After growth had taken place, the Teflon was cooled by water for 15 min. The sample was then rinsed in MiliQ water and dried in N₂. The growth solution was collected to measure its pH. Control experiments without the ZnO powders were also conducted to investigate their role in the growth of the C-layer. As-prepared samples were stored under atmosphere (21 ± 1 °C, Humidity: 50–70%).

Surface morphology images of the samples were obtained from a Quanta F400 85 field emission scanning electron microscope (FE-SEM). Their microstructures were investigated using the transmission electron microscope (TEM, Philips, CM 20). To prepare the TEM sample, firstly, a drop of ethanol was dropped on a piece of the ITO-supported UCL-Ag-NA. Then, a Cu grid (covered with an ultrathin carbon film) was placed on it. Next, the Cu grid was moved across the surface of the ITO glass using forceps. The UCL-encapsulated Ag nanoparticles could be attached to the surface of the Cu grid. The ultraviolet/visible (UV/Vis) absorption spectra were measured using a Varian 50 Conc UV/Vis spectrophotometer. X-ray photoelectron spectroscopy (XPS) was carried out on an XPS (PHI Model 5802) with Al K_α radiation and calibrated by C1s at 284.6 eV. Raman spectra were measured using the micro Raman system (RM 3000 Renishaw) with confocal microscopy. To evaluate their SERS performance, rhodamine 6G (R6G, 10⁻⁶ M in water) and methylene blue (MB, 10⁻⁶ M in water) were used as target molecules. 5,10,15,20-Tetra(4-pyridyl)-21H,23H-porphine (TPP, Sigma Aldrich) was used to test the effect of hydrophobic molecules on the SERS signal. The samples were immersed in the target molecule solutions for 2 h before measurements were taken. A laser (514.5 nm, spot diameter: 1 μm) was used and the acquisition time was 10 s. The laser power was 25 mW × 0.5% for R6G, MB, and TPP except as otherwise stated. Ten different spots of each sample were randomly chosen for examination.

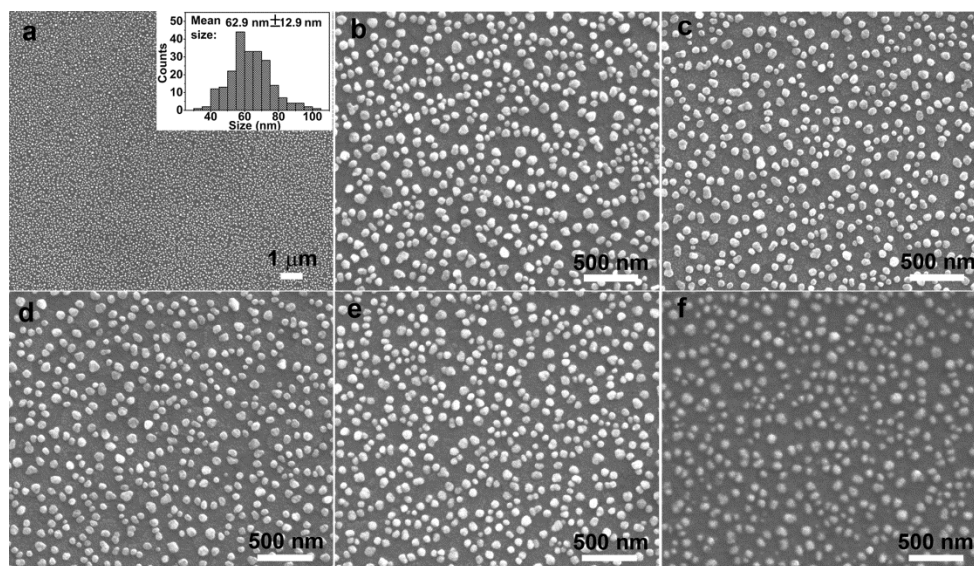


Fig. 1 (a-b) SEM images of Ag NA with different magnifications; (c-f) SEM images of UCL-Ag-NA with different C-layer growth time; (c) 2.7 h, (d) 3 h, (e) 4 h, and (f) 5 h. The inset in (b) is the size diagram of the Ag nanoparticles.

3. Results and discussion

Figs. 1a and b show the surface morphology of the Ag NA on ITO glass, revealing the large area of uniformity. The quick nucleation and slow growth process, as controlled by the double-potentiostatic

method, contributed to the good uniformity.⁹ Figs. 1c-e show the SEM images of the UCL-Ag-NA with C-layers grown for different lengths of time and adding ZnO powders. It can be seen that no obvious change can be observed as the growth time of the UCL goes from 2.7 h to 4 h. However, after growing for 5 h, a blurry SEM

image is obtained, as shown in Fig. 1f, which may result from the decreased electron conductivity obtained by coating relatively a thicker UCL. Figs. 2a-d show the TEM images of UCL–Ag–NA with C-layers grown for different lengths of time. When the growth time is 2.7 h, no obvious C-layer can be observed. This is caused by the fact that there is little difference between the C-layer and the C

film on the Cu grid. As the growth time increases from 3 h to 5 h, the thickness of the C-layer also increases. The average thicknesses of the C-layers as grown for 3 h, 4 h, and 5 h are measured as 4.5 ± 0.8 , 7.3 ± 1.5 , and 10.5 ± 1.5 nm, respectively.

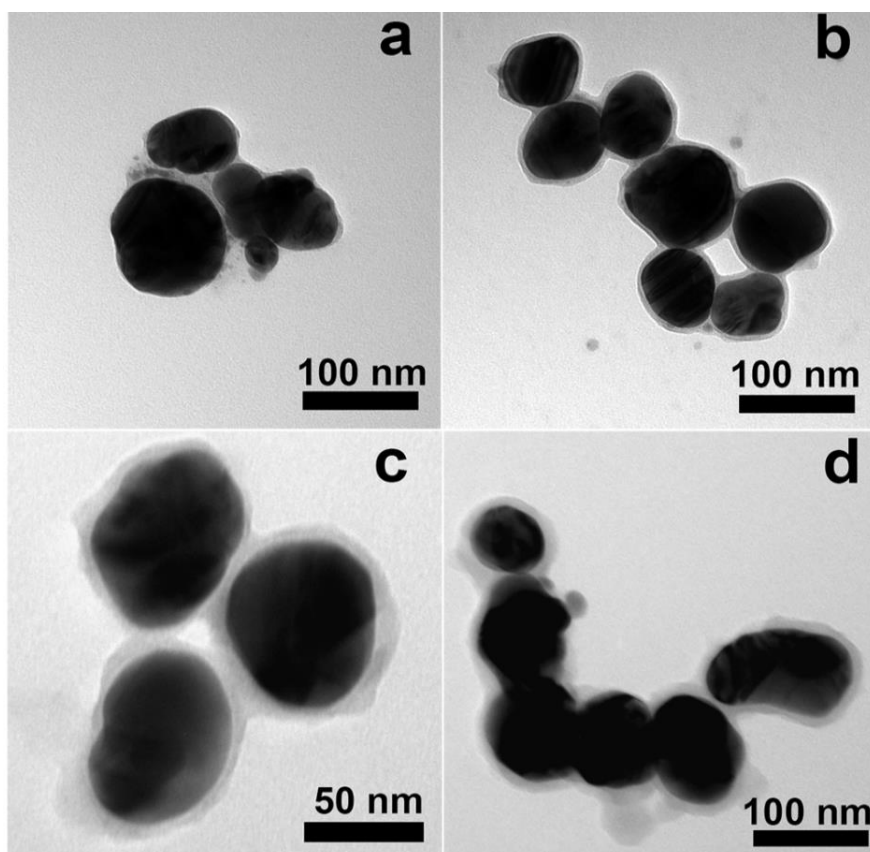


Fig. 2 (a-d) TEM images of UCL–Ag–NA with different C-layer growth times; (a) 2.7 h, (b) 3 h, (c) 4 h, and (d) 5 h.

Fig. 3 presents the XPS spectra of the UCL–Ag–NA. From Fig. 3a, sharp Ag peaks without oxidized states are found. In Fig. 3b, the C1s peak is fitted into four peaks, including C=C/CH_x/C–C, C=O, and –COOR peaks. These are characteristic peaks of C materials formed hydrothermally from glucose.¹⁸

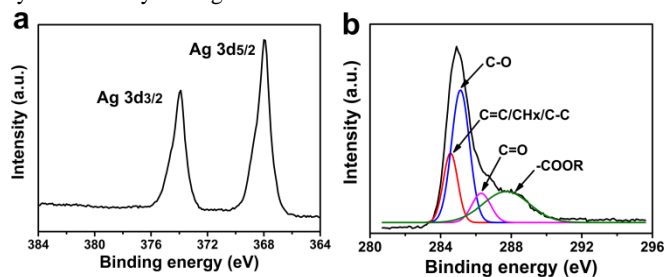


Fig. 3 XPS spectra of (a) Ag 3d and (b) C 1s peaks of UCL–Ag–NA grown for 3 h.

It can be seen that if no ZnO powders were added to the C-layer growth solutions, most of the Ag nanoparticles dissolved under hydrothermal conditions. SEM images of the Ag NA grown for 2.7 h, 3 h, and 4 h without ZnO powders are shown in Figs. 4a-c. The density of the Ag nanoparticles decreases from $7.8 \times 10^9 \text{ cm}^{-2}$ to $9.4 \times 10^8 \text{ cm}^{-2}$, $6.0 \times 10^8 \text{ cm}^{-2}$, and $4.6 \times 10^8 \text{ cm}^{-2}$ after growing for 2.7 h, 3 h, and 4 h, respectively, as shown in Figure 4d. By measuring

the pH values of the solutions after the hydrothermal reaction, as shown in Fig. 4e, it can be seen that the solution becomes acidic, indicating the formation of acid. A longer growth time leads to a lower pH. It has been reported that the decomposition of glucose gives rise to the formation of organic acids such as lactic, acetic, formic, etc, which decrease the pH value of a solution.¹⁷ When the ZnO powders are added, the reaction produces a nearly neutral solution. It is well known that ZnO is sensitive to the pH value of a solution. It is easily corroded in aqueous solutions with $\text{pH} < 5$. The acids formed during a hydrothermal reaction can react with ZnO, leading to a stable pH value. Hence, it is confirmed that the acidic conditions cause the corrosion of the Ag nanoparticles.

Fig. 5 shows the UV/Vis absorption spectra of the Ag NA and UCL–Ag–NA. Both the dipole (around 450 nm) and the quadrupole (around 360 nm) modes of the Ag nanoparticles exhibit red shifts as the thickness of the C-layer increases.¹⁹ Reports confirm that LSP resonance peaks are sensitive to small changes in the dielectric environment around the metal nanostructures, making them potentially good biosensors. Under the same conditions (e.g. thickness), metal nanostructures coated with different materials present different resonance peak shifts, due to the change in the refractive index.²⁰ For the same material, an increase in the film thickness can also lead to an incremental red shift in the resonance peak because of the enhanced damping of the LSP. The shift of the resonance peaks can be up to 300 nm for the TiO₂ layer coating.²⁰

Hence, it is reasonable that a C-layer of about 10.5 nm results in a peak shift of 60 nm.

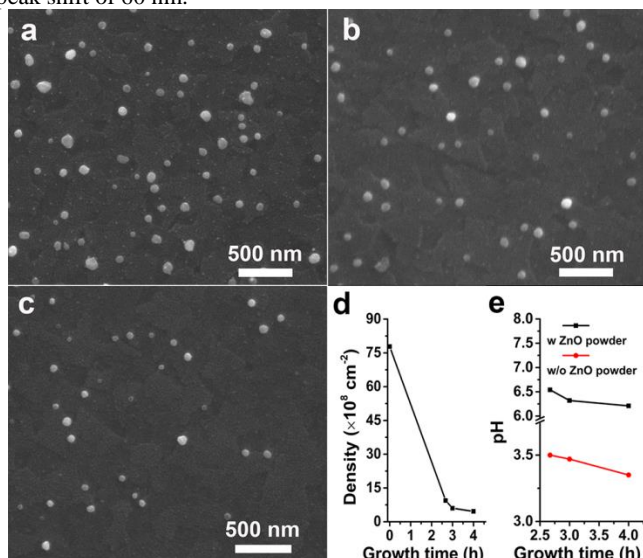


Fig. 4 SEM images of Ag NA after growing the C-layer for (a) 2.7 h, (b) 3 h, and (c) 4 h without adding ZnO powders; (d) Density of Ag nanoparticles after C-layer growth without adding ZnO powder; (e) pH values of the C-layer growth solutions with and without ZnO powder versus growth time.

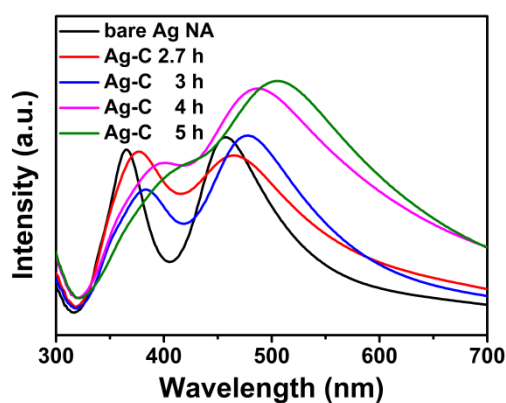


Fig. 5 Absorption spectra of UCL-Ag-NA with different C-layer growth times.

To investigate the effect of C-layer thickness on the SERS signal, the Raman spectra of R6G molecules adsorbed on the surface of UCL-Ag-NA with different C-layer thicknesses were examined as shown in Fig. 6a. It can be seen that the enhancement ability of the UCL-Ag-NA gradually declines as the thickness of the C-layer increases. No SERS signal can be detected when the C-layer is about 10.5 nm. This confirms that SERS is a form of near-field phenomenon caused mainly by the strong surface electric field produced by plasmonic nanostructures under excitation.

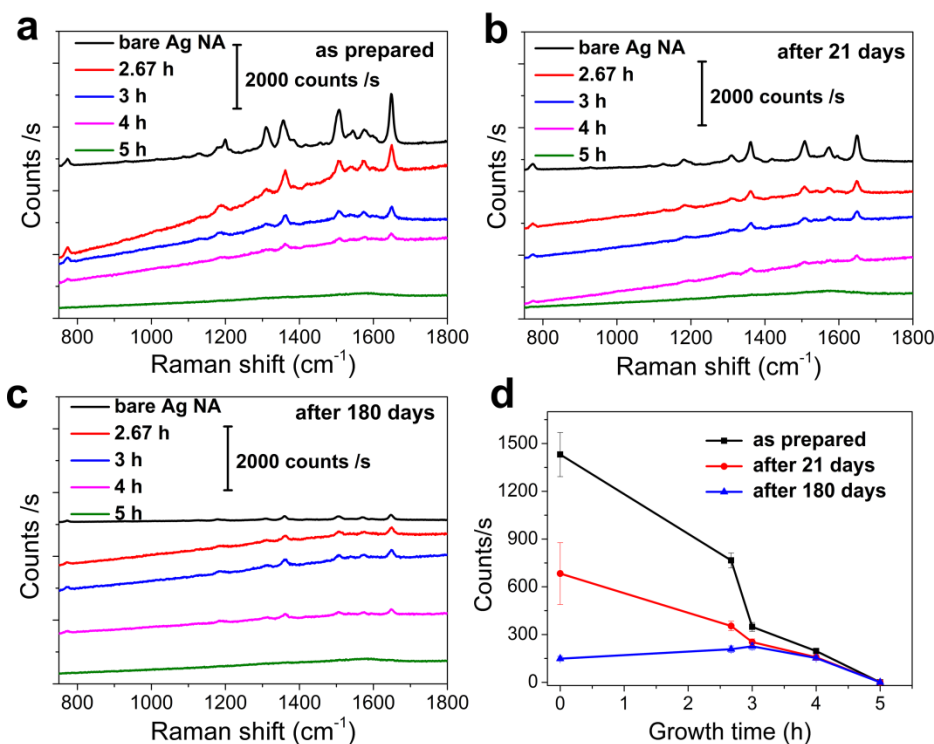


Fig. 6 The SERS spectra of R6G molecules adsorbed on the surface of (a) as prepared, (b) 21 days stored, and (c) 180 days stored Ag NA and UCL-Ag-NA with different growth times; (d) Change of Raman intensity of 1651 cm^{-1} obtained from as prepared, 21 days stored, and 180 days stored Ag NA and UCL-Ag-NA versus C-layer growth time.

In this work, it is shown that the C-layer weakens the electric field around the target molecules. On the one hand, a thicker C-layer decreases the surface electric field intensity of the Ag nanoparticles.¹³ On the other, it also separates the target molecules farther from their surfaces. As a result, the intensity of the SERS signal reduces as the thickness of the C-layer increases. As it is

difficult to prevent the formation pinholes in the C-layer, it is possible that the molecules adsorbed in the pinhole give stronger Raman signals than those on the surface. Moreover, with a prolonged growth time, the standard deviation of the C-layer thickness increases, which may also be a factor affecting the SERS signal intensity.

To evaluate their durability for SERS applications, the Raman spectra of R6G molecules adsorbed on the UCL–Ag–NA exposed to the atmosphere for 21 days and 180 days were examined as shown in Figs. 6b and c. After 21 days, the bare Ag NA still shows the best SERS performance. The enhancement ability of the UCL–Ag–NA is gradually weakened as the thickness of the C-layer increases. However, when they are stored for 180 days, the enhancement ability of bare Ag NA is less than that of the UCL–Ag–NA. To demonstrate a clear change in the Raman intensity versus C-layer thickness and storage time, the peak intensity of R6G centered at around 1651 cm^{-1} measured from UCL–Ag–NA with different C-layer thickness and storage time is monitored as shown in Fig. 6d. After 21 days' storage, the Raman intensity of R6G molecules adsorbed on bare Ag–NA, UCL(<4.5 nm)–Ag–NA, UCL(4.5 nm)–Ag–NA, UCL(7.3 nm)–Ag–NA, and UCL(10.5 nm)–Ag–NA are about 10.4%, 27.2%, 64.9%, and 77.8% of those obtained from their fresh counterparts. For the fresh samples, after growing the C-layer for 3 h and 4 h, the Raman signal intensity decreases to 24.3% and 13.7% of that obtained from bare Ag NA. However, after 180 days' storage, their SERS signal intensity becomes 152.7% and 102.9% of that obtained from bare Ag NA stored for 180 days, indicating that they perform better after prolonged storage. The SERS intensity of the bare Ag NA after 180 days' storage is 10.3% of that of its fresh counterpart. In contrast, UCL(<4.5 nm)–Ag–NA has poor stability, which may be attributable to the C-layer being too thin. UCL(4.5 nm)–Ag–NA and UCL(7.3 nm)–Ag–NA have better durability, as more than 60% of the SERS signal intensity is maintained. The Raman spectra of R6G adsorbed on the surface of Ag NA after the hydrothermal growth of a C-layer without ZnO powders was also studied (Fig. S1). The peak intensity at around 1651 cm^{-1} for the growth times of 2.7 h, 3 h, and 4 h decreases to 6.5%, 4.5% and 2.9%, respectively, of that obtained from the as-prepared Ag NA.

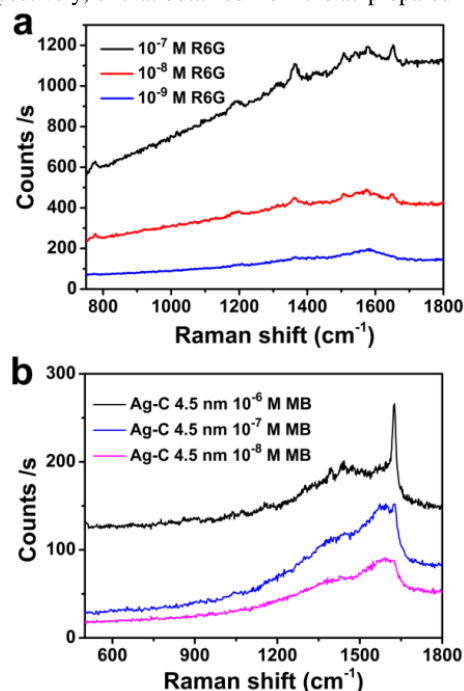


Fig. 7 SERS spectra of MB molecules adsorbed on the surface of UCL–Ag–NA with C-layer growth times of 3 h and 4 h.

Although this improvement in the durability of UCL–Ag–NA is not dramatic, it is still potentially valuable for some applications. For example, in living systems, for the reliable detection of signals over a short period, the SERS substrate should be relatively stable in the host and should not cause it any harm.²¹ For bare Ag-based SERS

substrate, the surface Ag₂O layer can be corroded in the host and release Ag⁺, which is harmful. The UCL can protect the Ag-based SERS substrate from oxidation and corrosion under *in vivo* conditions. The durability of UCL–Ag–NA enables a reliable signal. To further investigate the enhancement ability of the UCL–Ag–NA, SERS spectra of the R6G molecules with different concentrations were measured as shown in Fig. 7a. The concentration limit is up to the 10^{-8} M scale. MB, a nonresonance molecule under 514.5 nm excitation, was employed as an alternative target molecule to confirm the generality of the use of UCL–Ag–NA for different organics. From Fig. 7b, it can be seen that there are obvious MB peaks centered at around $1624, 1424, 1394, 504$ and 450 cm^{-1} .²² SERS spectra of MB molecules at different concentrations were also recorded. The lowest detectable concentration is 10^{-7} M , indicating the strong enhancement ability of the UCL–Ag–NA. Moreover, it is found that three-dimensional (3D) Ag nanostructures have stronger SERS enhancement ability than Ag NA.¹⁰ Therefore, by applying the methodology reported here, UCLs can be coated on the surface of 3D Ag nanostructures, resulting in a SERS substrate with improved durability. As a result, the detectable concentration of the target molecules can be further decreased compared with the UCL–Ag–NA in this work.

The surface of the Ag NA becomes more hydrophilic after coating with the UCL, as shown in Fig. S2. The hydrophobic molecule TPP was also tested (Fig. S3). It is found that its SERS signal is very weak, which can be ascribed to the poor adsorption force of TPP on the surface of the UCL–Ag–NA.

Although very broad SERS peaks are seen at around 1350 cm^{-1} and 1580 cm^{-1} in Fig. 7b, their intensity is very weak. When the SERS signal of the target molecules is strong, that of the C-layer can be omitted, as shown in Fig. 6a. Moreover, the peak width is much larger than that of the target molecules. Sharp peaks for the target molecules are obvious in the overlapped spectra, so it is easy to distinguish their signal from that of the C-layer.

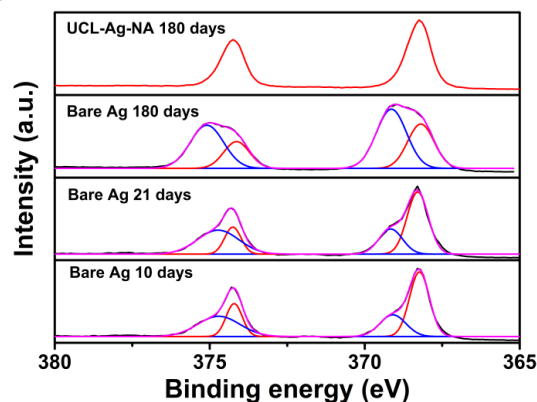


Fig. 8 XPS spectra of the Ag 3D peaks of bare Ag–NA and UCL(4.5nm)–Ag–NA after 180 days.

The XPS spectra of Ag NA stored for different periods (Fig. 8) show that the intensity of the Ag₂O increases with prolonged storage time,²³ illustrating the increase in the thickness of the Ag₂O layer. The TEM image of a typical Ag nanoparticle after 180 days of storage is shown in Fig. S4. The thickness of the Ag₂O is around 3 nm. This oxidation effect weakens the enhancement ability of the Ag NA. No oxidation state of Ag was found in the UCL–Ag–NA after 180 days of storage, indicating its effective role in preventing this deterioration. The decay in the SERS performance of the UCL–Ag–NA after 180 days of storage may be due to surface defects in the C-layer, which accords well with previous report.²⁴

4. Conclusions

UCL–Ag–NA as durable SERS substrates have been successfully fabricated on the surface of ITO glass using a hydrothermal method. The problem of the Ag NA dissolving during the hydrothermal process is solved by using ZnO powders. The pH values of the reacted solution demonstrate that the ZnO powders play the role of pH-buffering reagent. With an increase in the thickness of the C-layer, the SERS performance of the UCL–Ag–NA decreases, accompanied by improved stability of the Raman signal. The SERS signal intensity obtained from the UCL–Ag–NA with a C-layer of about 7.3 nm and stored for 180 days is 77.8% of that obtained from as-prepared counterparts. Without the C-layer, the SERS performance of the bare Ag NA declines with the increase of storage time, due to oxidation. UCL–Ag–NA can be employed as a durable SERS substrate. The methodology proposed in this work for C-layer coating can be used in Ag nanostructures of other dimensions to improve durability.

Acknowledgements

The work described in this paper was supported by a grant from the Research Grants Council of Hong Kong Special Administrative Region (SAR) [Project No. CityU 103812]. We also thank Professor Andrey L. Rogach for his help in this work.

Notes and references

^a Department of Physics and Materials Science and Centre for Functional Photonics (CFP), City University of Hong Kong, Hong Kong SAR, China.

^b Department of Physics, The Chinese University of Hong Kong, Hong Kong SAR, China.

† Electronic Supplementary Information (ESI) available: [details of any supplementary information available should be included here]. See DOI: 10.1039/b000000x/

References

- 1 W. L. Barnes, A. Dereux, and T. W. Ebbesen, *Nature*, 2003, **424**, 824–830.
- 2 P. A. Hobson, S. Wedge, J. E. Wasey, I. Sage, and W. L. Barnes, *Adv. Mater.*, 2002, **14**, 1393–1396.
- 3 H. Atwater and A. Polman, *Nat. Mater.*, 2010, **9**, 205–213.
- 4 S. R. E. S. Nie, *Science*, 1997, **275**, 1102–1106.
- 5 D. D. D. Ying Fang, Nak-Hyun Seong, *Science*, 2008, **321**, 388–393.
- 6 K. Kneipp and H. Kneipp, *Acc. Chem. Res.*, 2006, **39**, 443–450.
- 7 J. C. Bian, Z. D. Chen, Z. Li, F. Yang, H. Y. He, J. Wang, J. Z. Y. Tan, J. L. Zeng, R. Q. Peng, X. W. Zhang, and G. R. Han, *Appl. Surf. Sci.*, 2012, **258**, 6632–6636.
- 8 H. Wang, C. S. Levin, and N. J. Halas, *J. Am. Chem. Soc.*, 2005, **127**, 14992–14993.
- 9 J. C. Bian, Z. Li, Z. D. Chen, H. Y. He, X. W. Zhang, X. Li, and G. R. Han, *Appl. Surf. Sci.*, 2011, **258**, 1831–1835.
- 10 J. C. Bian, Z. Li, Z. Chen, X. Zhang, Q. Li, S. Jiang, J. He, and G. Han, *Electrochim. Acta*, 2012, **67**, 12–17.
- 11 A. Sánchez-Iglesias, P. Aldeanueva–Potel, W. Ni, J. Pérez–Juste, I. Pastoriza–Santos, R. a. Alvarez–Puebla, B. N. Mbenkum, and L. M. Liz-Marzán, *Nano Today*, 2010, **5**, 21–27.
- 12 R. T. Tom, A. S. Nair, N. Singh, M. Aslam, C. L. Nagendra, R. Philip, K. Vijayamohan, and T. Pradeep, *Langmuir*, 2003, **19**, 3439–3445.
- 13 J. F. Li, Y. F. Huang, Y. Ding, Z. L. Yang, S. B. Li, X. S. Zhou, F. R. Fan, W. Zhang, Z. Y. Zhou, D. Y. Wu, B. Ren, Z. L. Wang, and Z. Q. Tian, *Nature*, 2010, **464**, 392–395.
- 14 F. Liu, Z. Cao, C. Tang, L. Chen, and Z. Wang, *ACS Nano*, 2010, **4**, 2643–2648.
- 15 X. Li, J. Li, X. Zhou, Y. Ma, Z. Zheng, X. Duan, and Y. Qu, *Carbon*, 2014, **66**, 713–719.

- 16 Y. Zhang, C. Xing, D. Jiang, and M. Chen, *CrystEngComm*, 2013, **15**, 6305–6310.
- 17 W. Wu, G. Hu, S. Cui, Y. Zhou, and H. Wu, *Crystal Growth & Design*, 2008, **8**, 4014–4020.
- 18 M. Sevilla and A. B. Fuertes, *Chem. A Eur. J.*, 2009, **15**, 4195–4203.
- 19 D. D. Evanoff and G. Chumanov, *Chemphyschem*, 2005, **6**, 1221–1231.
- 20 G. Xu, M. Tazawa, P. Jin, S. Nakao, and K. Yoshimura, *Appl. Phys. Lett.*, 2003, **82**, 3811–3813.
- 21 D. A. Stuart, J. M. Yuen, N. Shah, O. Lyandres, C. R. Yonzon, M. R. Glucksberg, J. T. Walsh, and R. P. Van Duyne, *Anal. Chem.* 2006, **78**, 7211–7215.
- 22 S. H. Nicolai and J. C. Rubim, *Langmuir*, 2003, **19**, 4291–4294.
- 23 X. Wang, S. Li, H. Yu, J. Yu, and S. Liu, *Chem. An Eur. J.*, 2011, **17**, 7777–7780.
- 24 D. Li, S. Wu, Q. Wang, Y. Wu, W. Peng, and L. Pan, *J. Phys. Chem. C*, 2012, **116**, 12283–12294.